The Astrophysical Journal Letters, 843:L15 (7pp), 2017 July 1 https://doi.org/10.3847/2041-8213/aa7b2c

Sunspot Light Walls Suppressed by Nearby Brightenings

Shuhong Yang[1,2], Jun Zhang[1,2], Robertus Erdélyi[3,4], Yijun Hou[1,2], Xiaohong Li[1,2], and Limei Yan[5]
[1] CAS Key Laboratory of Solar Activity, National Astronomical Observatories, Chinese Academy of Sciences, Beijing 100012, China; shuhongyang@nao.cas.cn
[2] College of Astronomy and Space Sciences, University of Chinese Academy of Sciences, Beijing 100049, China
[3] Solar Physics and Space Plasma Research Centre, School of Mathematics and Statistics, University of Sheffield, Hicks Building, Hounsfield Road, Sheffield S3 7RH, UK
[4] Department of Astronomy, Eötvös Loránd University, P.O. Box 32, H-1518 Budapest, Hungary
[5] Key Laboratory of Earth and Planetary Physics, Institute of Geology and Geophysics, Chinese Academy of Sciences, Beijing 100029, China
Received 2017 June 6; revised 2017 June 20; accepted 2017 June 21; published 2017 June 30

Abstract

Light walls, as ensembles of oscillating bright structures rooted in sunspot light bridges, have not been well studied, although they are important for understanding sunspot properties. Using the *Interface Region Imaging Spectrograph* and *Solar Dynamics Observatory* observations, here we study the evolution of two oscillating light walls each within its own active region (AR). The emission of each light wall decays greatly after the appearance of adjacent brightenings. For the first light wall, rooted within AR 12565, the average height, amplitude, and oscillation period significantly decrease from 3.5 Mm, 1.7 Mm, and 8.5 minutes to 1.6 Mm, 0.4 Mm, and 3.0 minutes, respectively. For the second light wall, rooted within AR 12597, the mean height, amplitude, and oscillation period of the light wall decrease from 2.1 Mm, 0.5 Mm, and 3.0 minutes to 1.5 Mm, 0.2 Mm, and 2.1 minutes, respectively. Particularly, a part of the second light wall even becomes invisible after the influence of a nearby brightening. These results reveal that the light walls are suppressed by nearby brightenings. Considering the complex magnetic topology in light bridges, we conjecture that the fading of light walls may be caused by a drop in the magnetic pressure, where the flux is canceled by magnetic reconnection at the site of the nearby brightening. Another hypothesis is that the wall fading is due to the suppression of driver source (*p*-mode oscillation), resulting from the nearby avalanche of downward particles along reconnected brightening loops.

Key words: Sun: chromosphere – Sun: photosphere – Sun: UV radiation – sunspots

Supporting material: animations

1. Introduction

Light bridges are bright structures deeply anchored in the convection zone, and they are often accounted for the incompletely suppressed convection (Sobotka et al. 1993; Borrero & Ichimoto 2011; Lagg et al. 2014). The magnetic field in a light bridge is mostly much weaker than the neighboring umbra (Rueedi et al. 1995; Jurčák et al. 2006; Sobotka et al. 2013). Analyzing images obtained in the 1600 Å ultraviolet (UV) channel of the *Transition Region and Coronal Explorer*, Berger & Berdyugina (2003) found persistent brightness enhancements over a light bridge. In some other studies, more dynamic brightenings and surges were observed in the lower atmosphere above sunspot light bridges (Asai et al. 2001; Shimizu et al. 2009; Louis et al. 2014; Tian et al. 2014; Toriumi et al. 2015a, 2015b; Robustini et al. 2016; Song et al. 2017).

Combining observations of AR 12192 made by the *New Vacuum Solar Telescope* (Liu et al. 2014) and *Interface Region Imaging Spectrograph* (*IRIS*; De Pontieu et al. 2014), Yang et al. (2015) found an ensemble of oscillating bright structures rooted in a light bridge and named it *light wall*. The light wall, especially the wall top, is much brighter than the surroundings. Yang et al. (2015) suggested that the light-wall oscillations are caused by the leakage of *p*-modes from the subphotosphere. Bharti (2015) also noted that a wave phenomenon seems to be responsible for the coherent behavior of neighboring oscillating structures above the light bridge. Afterward, a survey of seven-month *IRIS* observations by Hou et al. (2016a) reveals that most light walls are rooted in light bridges. Recently, Zhang et al. (2017) analyzed *IRIS* spectral data of a light wall that also exhibits pronounced oscillations in the height of the light wall. They deduced from the blueshifted and redshifted Doppler signals that the oscillations are likely caused by shocked *p*-mode waves originated from the subphotosphere.

Last but not least, Yang et al. (2016) found that when falling material reached the base of a light wall the height and brightness of the light wall increased, implying that the light wall can be enhanced by an external disturbance. Different from the light-wall enhancement, we report in the present Letter an unusual and puzzling phenomenon, i.e., light walls can be significantly weakened due to the suppression of nearby brightenings observed by *IRIS* and the *Solar Dynamics Observatory* (*SDO*; Pesnell et al. 2012).

2. Observations and Data Analysis

We study two light walls suppressed by nearby brightenings. The first event (Event 1) was observed by *IRIS* from 22:04:13 UT on 2016 July 22 to 02:08:33 UT on July 23 with a cadence of 37 s. The second one (Event 2) was also observed by *IRIS* from 12:01:52 UT to 19:30:10 UT on 2016 September 26 with a cadence of 21 s. For each event, there are four series of images obtained with a slit-jaw imager (SJI) in 2832, 2796, 1330, and 1400 Å channels. These SJI images have a pixel size of 0.″333 and a field of view (FOV) of 120″ × 119″. The Atmospheric Imaging Assembly (AIA; Lemen et al. 2012) on board *SDO* monitors the Sun in 10 (E)UV lines with a pixel size of 0.″6 and a cadence of (12)24 s. For these two events, we mainly focus on two sequences of AIA 94 Å images in order to study the loop brightenings near the light walls. To coalign the *IRIS* images with the AIA intensity maps, we use concurrently

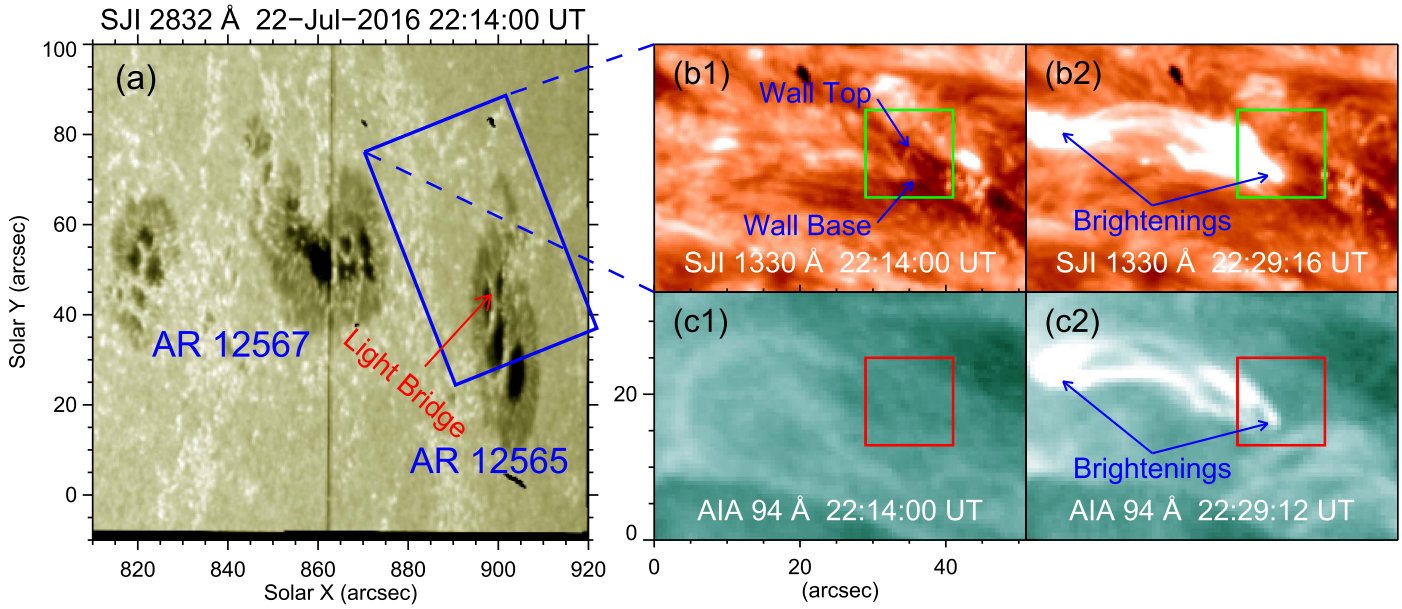

Figure 1. Panel (a): *IRIS*/SJI 2832 Å image taken on 2016 July 22. The blue rectangle outlines the FOV of panels (b1)–(c2), and the red arrow denotes a light bridge within a sunspot of AR 12565. Panels (b1)–(b2): SJI 1330 Å images showing a light wall rooted in the light bridge and the nearby brightenings. Panels (c1)–(c2): *SDO*/AIA 94 Å images displaying the EUV appearance corresponding to panels (b1) and (b2) (see also the animation). The blue arrows in panel (b1) indicate the top and base of the light wall, and the blue arrows in panels (b2) and (c2) denote the brightening loop set. The squares outline the FOV of Figures 2(a1)–(b3).

(An animation of this figure is available.)

taken continuum images from the Helioseismic and Magnetic Imager (HMI; Scherrer et al. 2012) on board *SDO*. Each sequence of the *SDO* data is processed to Level 1.5 by applying the standard routine aia_prep.pro and then differentially rotated to a reference time. Thus, the AIA and HMI images are automatically aligned. Next, we coalign the *IRIS* 2832 Å data with the HMI intensity maps using the cross-correlation method (setpts.pro available as part of the SSWIDL software tree).

3. Results

The first light wall is rooted in a light bridge (denoted by the red arrow in Figure 1(a)) within AR 12565, which is located at the west of AR 12567 and close to the west limb of the solar disk. At 22:14:00 UT, the light wall, especially the wall top and wall base (pointed by two arrows in panel (b1)) can be identified in the SJI 1330 Å image. At the left side, near the light wall, a set of loops with a length of about 25 Mm brightened, which were quite conspicuous at 22:29:16 UT (the footpoints of these loops are marked by arrows in panel (b2)). Since the appearance of the light wall and nearby brightenings in SJI 1400 Å images are similar to that in 1330 Å images, we do not show the 1400 Å images here. In the simultaneous AIA image, the loops were very bright in the EUV 94 Å line (panel (c2); also see the animation of Figure 1). The loop brightening corresponds to a B5.6 flare with the peak at 22:30 UT, according to the *Geostationary Operational Environmental Satellite* soft X-ray flare classification. However, the loops were invisible in 94 Å 15 minutes ahead (see panel (c1)).

Figures 2(a1)–(a3) and the associated animation show the light wall in SJI 2796 Å before, during, and after the influence of the nearby brightening, respectively. The corresponding appearances in SJI 1330 Å are presented in panels (b1)–(b3). The top and base of the light wall are identified from both the 1330 and 2796 Å images. At 22:23 UT, the projected height (the distance between the wall top and wall base) was about 2.1 Mm (see panels (a1) and (b1)). The nearby brightening extended to the light wall from the left side and then impacted on the wall base (panels (a2) and (b2)). After that, the light wall became much fainter and less pronounced, both in emission and height (panels (a3) and (b3)). To study the fading of the light wall, we derive two time–distance plots (see panels (c) and (d)) from two sequences of SJI 2796 and 1330 Å images along slice "A–B" (marked by blue dashed lines in panels (a2) and (b2)). From analyzing the time–distance plots in panels (c) and (d), we conclude that the wall top moved upward and downward successively, indicating an oscillatory pattern in the height of the light wall. At the time around 22:29 UT (marked by the vertical lines), the brightening nearby the wall (denoted by the blue arrow) began to affect the light wall. The average height of the light wall before this influence was about 3.5 Mm. Due to the influence caused by the brightening, the mean height of the light wall decreased to 1.6 Mm. The average amplitude of the associated oscillation also decreased, from 1.7 to 0.4 Mm. In addition, the oscillation period of the light wall has also changed. In the 18.5 minutes interval preceding the interaction with the brightening, the mean period of oscillation was about 8.5 minutes, and after the interaction, it has dropped down to about 3.0 minutes in the following 13 minute interval.

The second light wall is located within the emerging AR 12597 (see Figure 3(a)). We note that there is another light bridge (pointed by the red arrow in panel (a)) in one sunspot of the active region (AR). In the SJI 1330 Å image (panel (b)), a light wall rooted in the light bridge can be clearly identified, and its top and base are marked by two green arrows. However, the light wall was almost invisible in the AIA 94 Å image at 15:15:12 UT (panel (c1)). Several minutes later, a set of coronal loops with an average length of about 45 Mm brightened, i.e., that this is an estimated length, as highlighted by the arrows in panel (c2) (also see the animation of Figure 3).

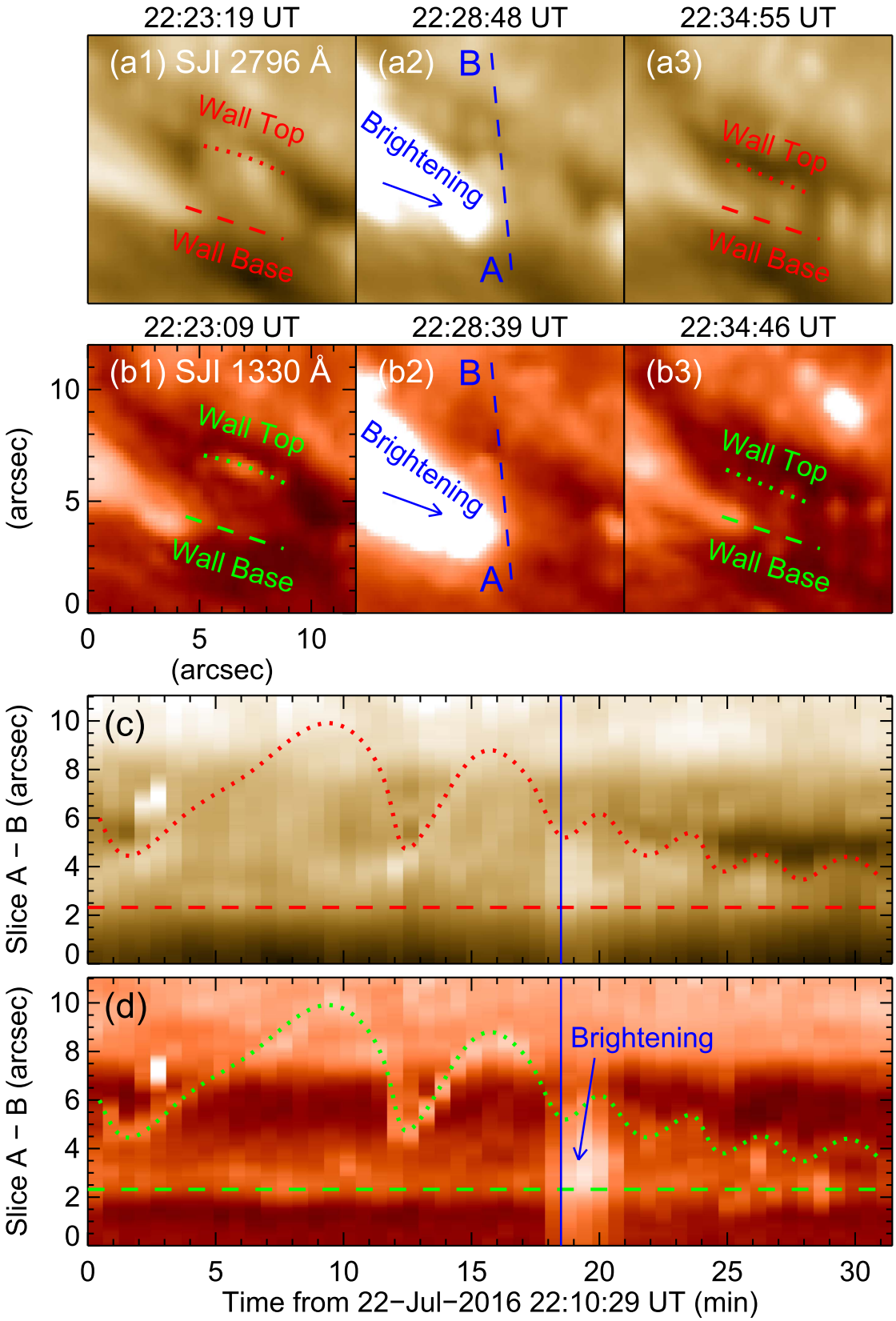

Figure 2. Panels (a1)–(a3): SJI 2796 Å images showing the evolution of the light wall under the influence of the brightening (marked by the blue arrow). Panels (b1)–(b3): similar to panels (a1)–(a3), but in the 1330 Å passband (see also the animation). The red/green dotted and dashed curves delineate the wall top and wall base, respectively. Panels (c)–(d): time–distance plots derived along slice "A–B" marked by the blue dashed lines in panels (a2) and (b2). The dotted curves and dashed lines outline the positions of the wall top and wall base, respectively. The vertical lines mark the moment of time when the brightening began to affect the light wall.

(An animation of this figure is available.)

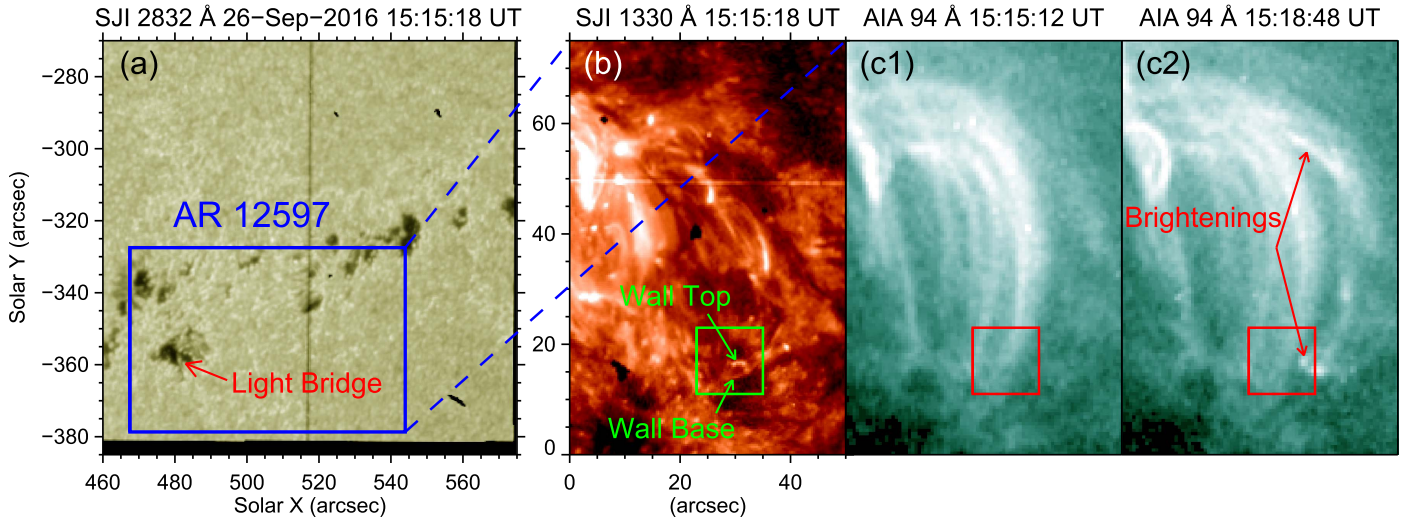

Figure 3. Panel (a): SJI 2832 Å image observed on 2016 September 26. The blue rectangle outlines the FOV of panels (b)–(c2), and the red arrow denotes a light bridge within a sunspot of AR 12597. Panel (b): SJI 1330 Å image displaying the light wall rooted in the light bridge. Panels (c1)–(c2): AIA 94 Å images showing the coronal appearance before and after the brightening of a set of loops (marked by the red arrows; see also the animation). The squares outline the FOV of Figure 4.

(An animation of this figure is available.)

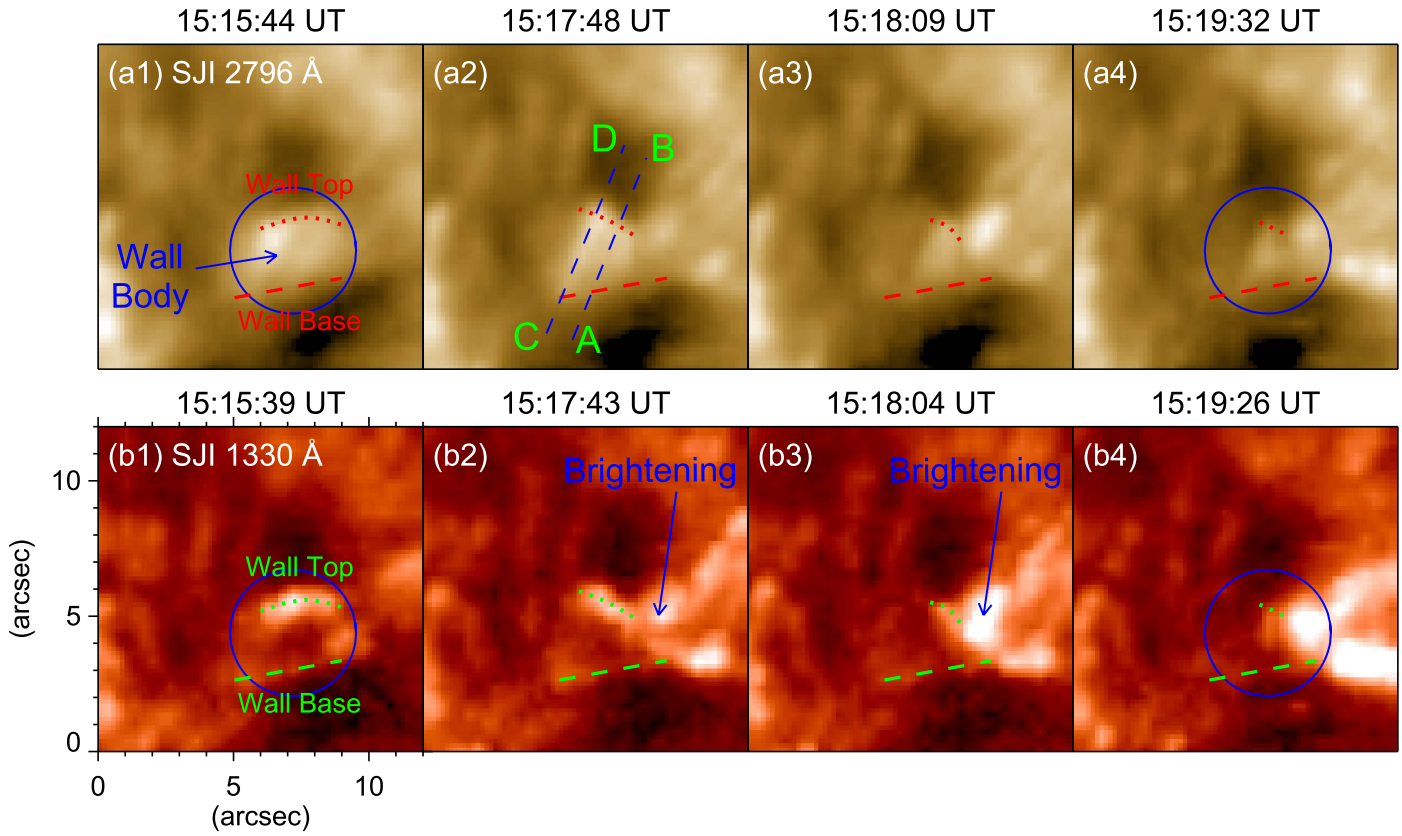

Figure 4. Panels (a1)–(a4): SJI 2796 Å image sequence showing the evolution of the light wall (encompassing area outlined by the blue circles). Panels (b1)–(b4): similar to panels (a1)–(a4), but in 1330 Å passband (see also the animation). The red/green dotted and dashed curves mark the wall top and wall base, respectively. The arrows in panels (b2) and (b3) denote the brightening close to the light wall. The blue dashed lines "A–B" and "C–D" in panel (a2) mark the positions where the time–distance diagrams shown in Figure 5 are obtained.

(An animation of this figure is available.)

The loop brightening corresponds to a B2.5 flare with the peak at 15:20 UT. We note that the loop set itself connects to the opposite polarity fields of the AR, and one of its ends appears as brighter points (marked by the lower arrow), located near the base of the light wall.

Figure 4(a1) shows that the light wall (outlined by the blue circle) is brighter than the surrounding area observed in SJI 2796 Å. In the SJI 1330 Å line, the emissions of the wall top and wall base are much higher than those of the wall body and the surrounding region (see panel (b1)). The right-side nearby

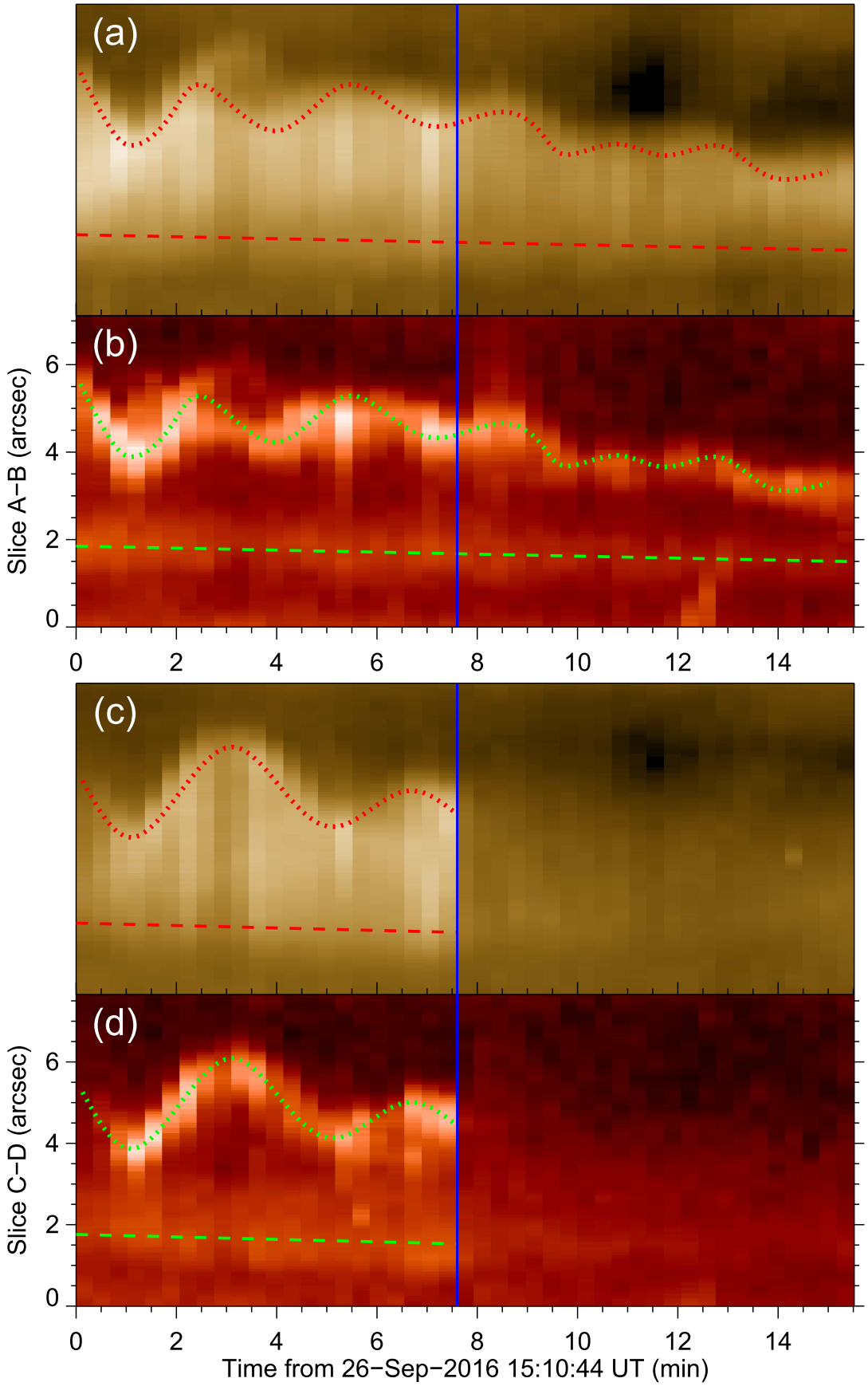

Figure 5. Panels (a)–(b): time–distance plots derived from the SJI 2796 Å and 1330 Å images along slice "A–B" marked in Figure 4. Panels (c)–(d): similar to panels (a) and (b), but along slice "C–D." The dotted curves mark out the top of the light wall, and the dashed lines approximate the wall base. The vertical lines indicate the moment of time when the light wall began to be suppressed by the nearby brightening.

region of the light wall brightened and was very appealing at 15:17:43 UT in SJI 1330 Å, as indicated by the arrow in panel (b2). Then, the brightening became more violent and affected the light wall at 15:18:04 UT, as shown in panels (a3) and (b3). The left part of the light wall (overlaid by slice "C–D") almost disappeared, and only the right part (overlaid by slice "A–B") remained (also see the animation of Figure 4). One and a half minutes later, the right part of the light wall became more faint in both 2796 and 1330 Å (see panels (a4) and (b4)).

In order to study the change of the light wall and to explore the corresponding cause(s) behind it, we construct the time–distance plots along slices "A–B" and "C–D" (marked in Figure 4(a2)), which cross the right and left parts of the light wall, respectively. Figures 5(a) and 5(b) are the time–distance plots obtained along slice "A–B" from SJI 2796 Å and 1330 Å, respectively. We can see that in the 7.5 minute interval before 15:18 UT (the start time of the brightening marked by the vertical line), the light wall (exactly the right part of the wall) was very bright, and its mean height was about 2.1 Mm. The mean amplitude and oscillation period were about 0.5 Mm and 3.0 minutes, respectively. After the influence caused by the brightening, the light wall became less prominent, as, e.g., the wall height decreased to about 1.5 Mm; the mean amplitude became 0.2 Mm and the oscillation period dropped down to around 2.1 minutes in the following 8 minutes. Along slice "C–D," two time–distance plots, derived from the SJI 2796 and 1330 Å images, are presented in Figures 5(c) and (d), respectively. The light wall (in particular, the left part of the wall) before 15:18 UT appeared as a bright oscillating structure with the oscillation period of about 4 minutes. Finally, after 15:18 UT, the light wall suddenly disappeared.

4. Conclusions and Discussion

Using *IRIS* and *SDO* multi-wavelength observations, we studied here two oscillating light walls within two ARs. Due to the influence of nearby brightenings, the brightness of each light wall decayed greatly. For the first light wall, rooted within AR 12565, the average height, amplitude, and oscillation period significantly decreased from 3.5 Mm, 1.7 Mm, and 8.5 minutes to 1.6 Mm, 0.4 Mm, and 3.0 minutes, respectively. For the second light wall, rooted within AR 12597, the mean height, amplitude, and oscillation period of the right part of the light wall decreased from 2.1 Mm, 0.5 Mm, and 3.0 minutes to 1.5 Mm, 0.2 Mm, and 2.1 minutes, respectively. In particular, the left part of the second light wall became invisible after the influence of the nearby brightening. Our results imply that these two light walls are suppressed by nearby brightenings.

In the study of Hou et al. (2016b), a light wall in AR 12403 was disturbed by an eruptive flare. The light wall was suggested to share a group of magnetic lines with the flaring loops, and the height variation of the light wall was interpreted with the projection effect due to the inclination changes. The upward pushing of large-scale loops lets the light wall turn to the vertical direction, thus resulting in the increase of the projective height of the wall. Afterward, the formation of low-lying post-flare loops makes the light wall seem to be lower in projection since the light wall inclined. However, in the present study, there are only some loop brightenings (denoted by the arrows in Figures 1(c2) and 3(c2)) instead of eruptive flares. The loop brightenings seem to be caused by magnetic reconnection among braided field lines, which is different from the eruptive flares with dramatic inclination changes due to the rise of stretching lines and the formation of post-flare loops. Therefore, the cartoons in Hou et al. (2016b) cannot be used to explain the decreases of the height, amplitude, oscillation period, and brightness of the light walls studied in the present work.

Solar flares often eject material from the lower atmosphere into the corona, and some material may fall back to the solar surface. Yang et al. (2016) noted that when the falling material reaches the base of a light wall, the kinetic energy is converted to thermal energy. The heated material of the light wall let the wall itself be much brighter. The pressure at the wall base increases, which powers the light wall to reach greater heights. Different from the light-wall enhancement by falling material, our results in the present study reveal that the light walls are suppressed by nearby brightenings. Since the height of a light wall can be determined by the pressure at the wall base, applying the logic presented in Yang et al. (2016), one would expect here a pressure decrease caused by the nearby brightening. This decrease could be, e.g., due to a drop in the magnetic pressure, where flux is canceled by magnetic reconnection at the site of the nearby brightening. The intermittent reconnection may cause the changes of the light-wall oscillation periods. Another opinion may be that the decrease of light-wall properties (e.g., its height) is due to the suppression of the driver source (*p*-mode oscillation) itself, resulting from the nearby hit of downward bulk plasma along reconnected brightening loops. Recent studies have revealed that the magnetic fields in sunspot light bridges are quite complex (Louis et al. 2015; Toriumi et al. 2015a, 2015b; Yuan & Walsh 2016). For example, Toriumi et al. (2015a) found that, in the light bridge, the magnetic field lines are highly inclined (almost horizontal to the solar surface in the direction along the light bridge) and appear as serpentine or arched structures. Thus, here we propose that when the downward propagating bulk plasma hits the light bridge possessing a complex magnetic topology it not only can affect the impact site but also influences the nearby light wall rooted in the light bridge. However, the exact mechanism for the light wall fading is not yet clear, and to further explore we need more observations and (MHD) modeling.

We thank the referee for valuable comments and Dr. Hui Tian for helpful discussion. The data are used courtesy of the *IRIS* and *SDO* science teams. *IRIS* is a NASA small explorer mission developed and operated by LMSAL with mission operations executed at NASA Ames Research center and major contributions to downlink communications funded by ESA and the Norwegian Space Centre. This work is supported by the National Natural Science Foundations of China (11673035, 11533008, 11373004), the Youth Innovation Promotion Association of CAS (2014043). R.E. is grateful to STFC (UK) and the Royal Society for the support received in a number of grants. He also thanks the Chinese Academy of Sciences Presidents International Fellowship Initiative, grant No. 2016VMA045 for support received. L.M.Y. is supported by National Postdoctoral Program for Innovative Talents (grant BX201600159).

References

Asai, A., Ishii, T. T., & Kurokawa, H. 2001, ApJL, 555, L65
Berger, T. E., & Berdyugina, S. V. 2003, ApJL, 589, L117
Bharti, L. 2015, MNRAS, 452, L16

Borrero, J. M., & Ichimoto, K. 2011, LRSP, 8, 4
De Pontieu, B., Title, A. M., Lemen, J. R., et al. 2014, SoPh, 289, 2733
Hou, Y. J., Li, T., Yang, S. H., & Zhang, J. 2016a, A&A, 589, L7
Hou, Y. J., Zhang, J., Li, T., et al. 2016b, ApJL, 829, L29
Jurčák, J., Martínez Pillet, V., & Sobotka, M. 2006, A&A, 453, 1079
Lagg, A., Solanki, S. K., van Noort, M., & Danilovic, S. 2014, A&A, 568, A60
Lemen, J. R., Title, A. M., Akin, D. J., et al. 2012, SoPh, 275, 17
Liu, Z., Xu, J., Gu, B.-Z., et al. 2014, RAA, 14, 705
Louis, R. E., Beck, C., & Ichimoto, K. 2014, A&A, 567, A96
Louis, R. E., Bellot Rubio, L. R., de la Cruz Rodríguez, J., Socas-Navarro, H., & Ortiz, A. 2015, A&A, 584, A1
Pesnell, W. D., Thompson, B. J., & Chamberlin, P. C. 2012, SoPh, 275, 3
Robustini, C., Leenaarts, J., de la Cruz Rodriguez, J., & Rouppe van der Voort, L. 2016, A&A, 590, A57
Rueedi, I., Solanki, S. K., & Livingston, W. 1995, A&A, 302, 543
Scherrer, P. H., Schou, J., Bush, R. I., et al. 2012, SoPh, 275, 207
Shimizu, T., Katsukawa, Y., Kubo, M., et al. 2009, ApJL, 696, L66
Sobotka, M., Bonet, J. A., & Vazquez, M. 1993, ApJ, 415, 832
Sobotka, M., Švanda, M., Jurčák, J., et al. 2013, A&A, 560, A84
Song, D., Chae, J., Yurchyshyn, V., et al. 2017, ApJ, 835, 240
Tian, H., Kleint, L., Peter, H., et al. 2014, ApJL, 790, L29
Toriumi, S., Cheung, M. C. M., & Katsukawa, Y. 2015a, ApJ, 811, 138
Toriumi, S., Katsukawa, Y., & Cheung, M. C. M. 2015b, ApJ, 811, 137
Yang, S. H., Zhang, J., & Erdélyi, R. 2016, ApJL, 833, L18
Yang, S. H., Zhang, J., Jiang, F. Y., & Xiang, Y. Y. 2015, ApJL, 804, L27
Yuan, D., & Walsh, R. W. 2016, A&A, 594, A101
Zhang, J. W., Tian, H., He, J. S., & Wang, L. H. 2017, ApJ, 838, 2